Energy considering for predicting the micro-creep behavior in composites with application in microelectronic and optoelectronic/photonic devices

V. MONFARED*, S. DANESHMAND[a]
Department of Mechanical Engineering, Zanjan Branch, Islamic Azad University, Zanjan, Iran
[a]Department of Mechanical Engineering, Majlesi Branch, Islamic Azad University, Isfahan, Iran

A new model is proposed to predict the micro-creep behavior of the composites with application in microelectronic and optoelectronic/photonic devices based on energy formulation, equilibrium and fundamental equations with considering geometric relations. In the present model, obtaining the unknown parameters is easier than the available approaches. Predicting the creep parameters is very significant to design the optoelectronic and photonic composites with optical fibers. Moreover, investigation of the creep behavior is important for failure, fracture, fatigue, and creep resistance of the optoelectronic/photonic composites. Finally, excellent agreements are found between the obtained analytical and FEM results.

(Received January 10, 2015; accepted March 19, 2015)

Keywords: Optoelectronic/photonic composites, Energy formulation, Micro-creep, Equilibrium and fundamental equations, FEM, Analytical method

1. Introduction

The use of the optoelectronic/photonic composites is recently growing because of their applications in different industries. Consequently, an understanding of the micro-creep behavior and its mechanisms for the materials is important and necessary, because, the creep in the electrical and optoelectronic/photonic systems (devices), and optical fibers can be very dangerous. Creep in these systems can create the serious disturbances in the advanced systems. The increasing application of the optical fibers in the optoelectronic/photonic composites requires a thorough knowledge of their creep characteristics, creep resistances, and deformation mechanisms.

Many researchers have studied the steady state creep behavior by analytical, numerical and experimental methods. Substantial and important researches have been done concerning the creep of the reinforced materials and their applications analytically [1-8], numerically [9-11], and experimentally [12-17]. The study presented in reference [7] analyzes the optical 1-soliton in the hollow-core photonic crystal fibers in the presence of space-dependent inter-modal dispersion, detuning and fiber loss using Hirota's bilinear and ansatz methods, in which, the explicit optical bright 1-solitons have been reported. For example, Lee et al. [11] proposed easy and direct methodology for stress analysis and prediction of the steady state creep deformation of discontinuously reinforced metal matrix composites utilizing finite element method (FEM). Also, the detection of volatile organic compound of methanol, ethanol, isopropanol, and acetone vapour at room temperature employing undoped ZnO and Al-doped ZnO coated on the optical fiber core has been reported [17]. Recently as a different work, the creep behavior in the materials has been studied using atomic properties [18].

In this study, the micro-creep model of the optoelectronic/photonic composites is analytically simulated for predicting and preventing possible dangerous creep behavior in the composite devices based on energy formulation, equilibrium and fundamental equations, and geometric relations. FEM is used for validating the present analytical results. To validate the present analytical method and obtained results, the results of the present analytical and FE methods are compared with together by experimental data for a creeping metal matrix composite MMC. Metal matrix composite is selected to validate the obtained results because of the inaccessibility to the experimental data of the creeping optoelectronic/photonic composites.

2. Materials and methods

Here, an axisymmetric unit cell is considered for simulating a complete short fiber composite shown in Fig. 1. In the mentioned model supposed that a cylindrical fiber with a radius a and a length $2l$ is inserted in a coaxial cylindrical matrix with an outer radius b and a length $2l'$. The volume fraction and aspect ratio of the fiber are introduced by f and $s = l/a$ respectively. In addition, $k = l'a/lb$ is assumed as a parameter related to the geometry of the unit cell.

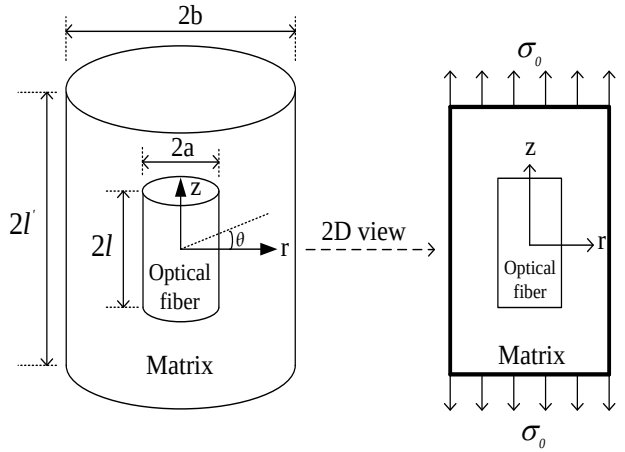

Fig. 1. Model of the unit cell.

An axial load "σ_0" is uniformly applied on the end faces of the unit cell (at $z=\pm l'$). The steady state condition is assumed. Elastic deformations are very small and are neglected in comparison with the creep deformations. The fiber and matrix have respectively elastic and plastic behaviors during the creep analysis. Material properties are assumed to be constant under applied load and temperature. The behavior of the creeping matrix is expressed by an exponential law as given in Eqs. (1, 2).

$$\tilde{F}(\sigma)=\Phi exp\left[\frac{\sigma_0}{\Lambda}\right] \tag{1}$$

$$\dot{\varepsilon}_e=\tilde{F}(\sigma) \tag{2}$$

In which, the parameters "Φ" and "Λ" are the material constants in the creeping matrix. These parameters are obtained by experimental methods for the steady state creep of the matrix. Moreover, σ_0 and $\dot{\varepsilon}_e$ are the equivalent stress and equivalent strain rates of the creeping matrix respectively. They are functions of *r* and *z*. Therefore, it turns out to be a very complex nonlinear time dependent problem. Then, the equilibrium equations in the cylindrical coordinate are introduced in the general form as the following,

$$\frac{\partial\sigma_r}{\partial r}+\frac{1}{r}\frac{\partial\tau_{r\theta}}{\partial\theta}+\frac{\partial\tau_{rz}}{\partial z}+\frac{1}{r}\left(\sigma_r-\sigma_\theta\right)+F_r=0 \tag{3}$$

$$\frac{\partial\tau_{r\theta}}{\partial r}+\frac{1}{r}\frac{\partial\sigma_\theta}{\partial\theta}+\frac{\partial\tau_{\theta z}}{\partial z}+\frac{2}{r}\tau_{r\theta}+F_\theta=0 \tag{4}$$

$$\frac{\partial\tau_{rz}}{\partial r}+\frac{1}{r}\frac{\partial\tau_{\theta z}}{\partial\theta}+\frac{\partial\sigma_z}{\partial z}+\frac{1}{r}\tau_{rz}+F_z=0 \tag{5}$$

This problem is axisymmetric, and then the equilibrium equations reduce to,

$$\frac{\partial\sigma_r(r,z)}{\partial r}+\frac{\partial\tau_{rz}(r,z)}{\partial z}+\frac{1}{r}\left(\sigma_r(r,z)-\sigma_\theta(r,z)\right)+F_r=0 \tag{6}$$

$$\frac{\partial\tau_{rz}(r,z)}{\partial r}+\frac{\partial\sigma_z(r,z)}{\partial z}+\frac{1}{r}\tau_{rz}(r,z)+F_z=0 \tag{7}$$

It is assumed that the body forces "F_r, F_θ and F_z" are small enough and may be zero. So, yields

$$\frac{\partial\sigma_r(r,z)}{\partial r}+\frac{\partial\tau_{rz}(r,z)}{\partial z}+\frac{1}{r}\left(\sigma_r(r,z)-\sigma_\theta(r,z)\right)=0 \tag{8}$$

$$\frac{\partial\tau_{rz}(r,z)}{\partial r}+\frac{\partial\sigma_z(r,z)}{\partial z}+\frac{1}{r}\tau_{rz}(r,z)=0 \tag{9}$$

The generalized fundamental equations for the steady state creep small deformation of the creeping matrix material in r,θ and *z* directions are the following forms,

$$\dot{\varepsilon}_r(r,z)=-\Gamma\left(\sigma_\theta(r,z)+\sigma_z(r,z)-\Delta\sigma_r(r,z)\right) \tag{10}$$

$$\dot{\varepsilon}_\theta(\mathrm{r,z})=-\Gamma\left(\sigma_\mathrm{r}(\mathrm{r,z})+\sigma_z(\mathrm{r,z})-\Delta\sigma_\theta(\mathrm{r,z})\right) \tag{11}$$

$$\dot{\varepsilon}_z(r,z)=-\Gamma\left(\sigma_r(r,z)+\sigma_\theta(r,z)-\Delta\sigma_z(r,z)\right) \tag{12}$$

In which, the parameter "Δ" is equal to 2 and parameter Γ is the following form,

$$\Gamma=\Omega\frac{\tilde{F}(\sigma)}{\sigma}=\Omega\frac{\dot{\varepsilon}_e}{\sigma_e}=\frac{\dot{\varepsilon}_e}{2\sigma_e} \tag{13}$$

$$\tilde{F}(\sigma)=\dot{\varepsilon}_e=\lambda\frac{\dot{\gamma}_{rz}\sigma_e}{\tau_{rz}} \tag{14}$$

Where, the parameter "λ" is constant and the equivalent stress σ_e is given by the following form,

$$\sigma_e=\frac{\sqrt{2}}{2}\left[0.67\left(\frac{\sigma_e\dot{\gamma}_{rz}}{\dot{\varepsilon}_e}\right)^2+\left(\sigma_r-\sigma_\theta\right)^2+\left(\sigma_r-\sigma_z\right)^2+\left(\sigma_z-\sigma_\theta\right)^2\right]^{\frac{1}{2}} \tag{15}$$

And also $\sigma_r,\sigma_\theta,\sigma_z$ and τ_{rz} are the stress components in the directions indicated by subscripts. Furthermore, $\dot{\varepsilon}_e$ is the equivalent strain rate and is described by Eqs. (1, 2 and 16), as the following,

$$\dot{\varepsilon}_e=\frac{\sqrt{2}}{3}\left[6\dot{\varepsilon}_{rz}{}^2+\left(\dot{\varepsilon}_r-\dot{\varepsilon}_\theta\right)^2+\left(\dot{\varepsilon}_r-\dot{\varepsilon}_z\right)^2+\left(\dot{\varepsilon}_z-\dot{\varepsilon}_\theta\right)^2\right]^{\frac{1}{2}} \tag{16}$$

Where, the parameters "$\dot{\varepsilon}_r,\dot{\varepsilon}_\theta,\dot{\varepsilon}_z$ and $\dot{\varepsilon}_{rz}$" are the strain rate components in the directions indicated by subscripts. In which, "λ, Ω and Δ" are equal to *0.34, 0.5* and *2* respectively. The strain rate-displacement rate relations are also given by the following,

$$\dot{\varepsilon}_r(r,z)=\frac{\partial\dot{u}(r,z)}{\partial r} \tag{17}$$

$$\dot{\varepsilon}_\theta(r,z)=\frac{\dot{u}(r,z)}{r} \tag{18}$$

$$\dot{\varepsilon}_z(r,z)=\frac{\partial \dot{w}(r,z)}{\partial z} \tag{19}$$

$$\dot{\gamma}_{rz}(r,z)=\frac{\partial \dot{u}(r,z)}{\partial z}+\frac{\partial \dot{w}(r,z)}{\partial r} \tag{20}$$

For the plastic-creep deformations (creeping material), each of the six stress-strain relations engaged is nonlinear and time dependent, and the strain-energy density in cylindrical coordinate at the any time may be expressed as,

$$\dot{\tilde{U}}=\frac{1}{2}\left[\sigma_r\left(\frac{\partial \dot{u}}{\partial r}\right)+\sigma_\theta\left(\frac{\dot{u}}{r}\right)+\sigma_z\left(\frac{\partial \dot{w}}{\partial z}\right)+\tau_{rz}\left(\frac{\partial \dot{u}}{\partial z}+\frac{\partial \dot{w}}{\partial r}\right)\right]+\dot{\bar{\alpha}}(r,z) \tag{21}$$

Also, for applied external load σ_0, the potential energy is as the following,

$$\Pi_{external}=-\int_R \rho b_i \dot{u}_i dV-\int_{\partial R_t}\sigma_z^a \dot{u}_i dS \tag{22}$$

Then, the external virtual work over a virtual displacement rate field $\delta\dot{u}$ is,

$$\delta W_{external}=-\delta\Pi_{external} \tag{23}$$

The principle of virtual work, then tells us that an elastic body is in equilibrium if and only if,

$$\delta\Pi=0 \tag{24}$$

In which,

$$\Pi=\Pi_{internal}+\Pi_{external} \tag{25}$$

That is, in the state of the equilibrium, the displacement rate field makes the total potential energy stationary with respect to virtual displacements. It can further be shown that for the equilibrium to be stable, the total potential energy must be a minimum. If Π is a local minimum, then, for any nonzero virtual displacement rate $\delta\dot{u}$ field $\Delta\Pi$, must be positive. In addition, the applied boundary conditions are given as the following,

$$\dot{u}(0,z)=0\ ,\ l\le z\le l' \tag{26}$$

$$\dot{u}(b,z)=\dot{u}_b\ ,0\le z\le l' \tag{27}$$

$$\dot{w}(r,0)=0, a\le r\le b \tag{28}$$

$$\dot{w}(a,z)=0 \tag{29}$$

$$\tau_{rz}(b,z)=\dot{\gamma}_{rz}(b,z)=0 \tag{30}$$

Also, the displacement rate at the outer surface, $\dot{u}_b$, (at $r = b$) is determined by the following relation,

$$\dot{\varepsilon}_e|_{r=b}=\Phi exp\left[\frac{\sigma_0-\left(k^n\times f^{2n}\times s^{2n+2}\right)}{\Lambda}\right],\ n=2 \tag{31}$$

After simplifying the results, for the normalized axial displacement rate have,

$$\dot{w}(b,z)\Big|^{r=b}_{\text{normalized axial displacement rate(present work)}}=8.35\times\left(\frac{z}{l}\right) \tag{32}$$

$$\dot{w}(b,z)\Big|^{r=b}_{\text{normalized axial displacement rate (FEM)}}=7.6\times\left(\frac{z}{l}\right)+0.0033 \tag{33}$$

Also, for normalized radial displacement rate have,

$$\dot{u}(b,z)\Big|^{r=b}_{\text{normalized radial displacement rate (FEM)}}=3\times10^{-15}\times\left(\frac{z}{l}\right)-1.11 \tag{34}$$

$$\dot{u}(b,z)\Big|^{r=b}_{\text{normalized radial displacement rate (present work)}}=-1 \tag{35}$$

It should be mentioned that the relation between the axial and radial displacement rates is according to the following formulation,

$$\dot{\varepsilon}_r(r,z)+\dot{\varepsilon}_\theta(r,z)+\dot{\varepsilon}_z(r,z)=\frac{\partial \dot{u}(r,z)}{\partial r}+\frac{\dot{u}(r,z)}{r}+\frac{\partial \dot{w}(r,z)}{\partial z}=0 \tag{36}$$

Also, Eq. (36) is known as the incompressibility condition that must be satisfied for the plastic deformations. Moreover, Eqs. (32-35) are determined using the combination of the energy formulations (Eqs. (21-25)), equilibrium and fundamental equations (Eqs. (1-16, 31,36)), and geometric relations (Eqs. (17-20)) with considering the applied boundary conditions (Eqs. (26-30)).

3. Results and discussions

For validation of the present method, the short fiber composite *SiC/6061Al* is selected as a case study and the obtained analytical and numerical results are compared with together. In which, steady state creep behavior of silicon carbide whisker/6061 aluminum composite has been studied at *300° C* under constant stress [12]. For the composite used here (*SiC/Al6061*), the volume fraction (*f*) of fibers is *15%* and the fibers have an aspect ratio (*s*) of *7.4* and *k = 0.76* [12]. Also, the steady state creep constants of the matrix material, "Φ" and "Λ", in Eq. (1) are considered as $\Phi = exp\ (-24.7)$ and $\Lambda = 6.47$ [12]. The following figures show the creep behaviors at the outer surface (*r=b*) in the second stage creep of the short fiber composites. Also, the axisymmetric unit cell model is considered for FEM creep analyzing.

The results obtained from the present method are presented in the following figures (see Figs. 2, 3). As mentioned before (inaccessibility to the experimental data of the creeping optoelectronic/photonic composites), for comparing the results of the present method, the

SiC/6061Al composite is chosen as a case study and also the determined analytical and numerical results are compared with together.

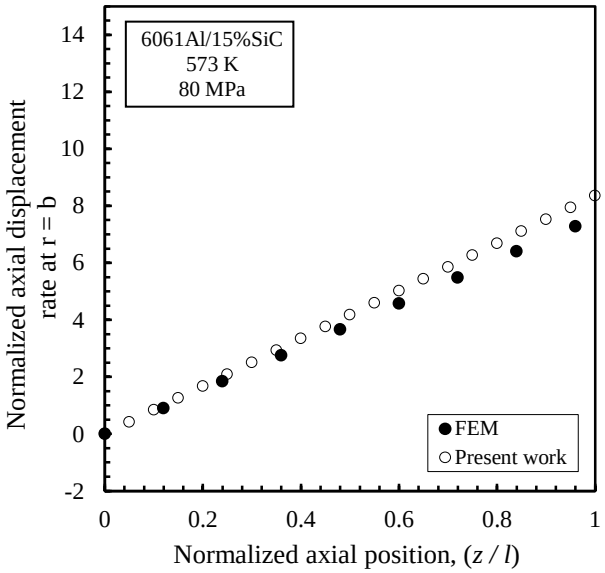

Fig. 2. Linear behavior of the axial displacement rate at r = b.

Fig. 2 shows smooth and uniform gradient in the axial displacement rate behavior at the outer surface of the unit cell in the steady state creep of the short fiber composites. That is, the mentioned behavior is related to the creeping matrix at the outer surface of the unit cell in the short fiber composites.

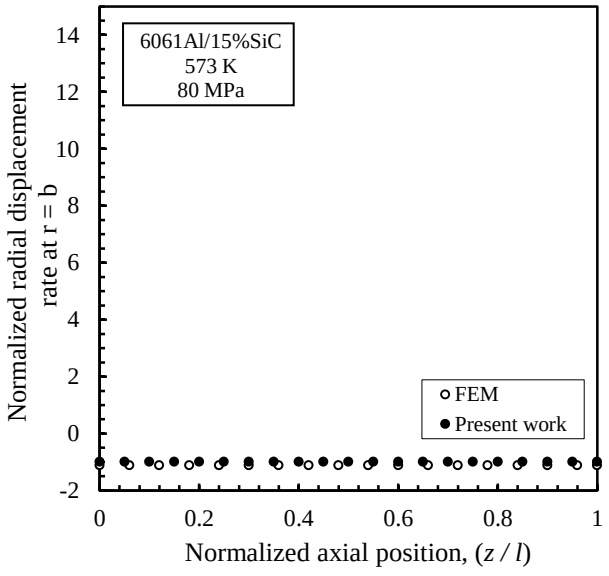

Fig. 3. Linear behavior of the radial displacement rate at r = b.

Slow and soft behaviors are also seen in Fig. 3 due to the steady state creep of the short fiber composite. That is, these behaviors are desirable and controllable. Also, we can control these behaviors by the obtained relations presented in Eqs. (32-35). According to the Figs. 2, 3, linear behaviors are observed in the radial and axial displacement rate behaviors in the steady state creep of the short fiber composites. That is, linear behavior with constant slope and gradient is seen in the axial and radial displacement rate behaviors at the outer surface ($r = b$). These linear behaviors are because of the nature of the tensile steady state creep and rate dependent small deformations. In these figures, good and proper compatibilities and agreements are found between finite element method (FEM) and present analytical work results for predicting the creep behaviors. Therefore, we can control the creep displacement rates in the optoelectronic/photonic composites with optical fiber using the present analytical method. Also, with this creep prediction, we can prevent from dangerous and undesirable events arising from the creep phenomenon in the optoelectronic/photonic composite devices with optical fiber.

4. Summary and conclusion

In this paper, for analyzing the micro-creep in the optoelectronic/photonic composite devices, a new analytical method was introduced to predict the creep behavior of the short fiber composites based upon energy formulations, equilibrium and fundamental equations, and geometric relations. Acceptable agreements were found between the numerical and analytical results. According to the obtained results, the following conclusions can be concluded,

- We can control the creep displacement rate behaviors in the optoelectronic/photonic composite devices with optical fiber by means of the present analytical method. Moreover, with the creep predicting, we can prevent from hazardous and unwelcome events arising from the happening the creep phenomenon in the optoelectronic/photonic composite devices with optical fiber.
- Uniform gradient is seen in the axial and radial displacement rate behaviors at the outer surface. So, these behaviors are controllable.
- Linear behavior with constant slope and gradients are observed in the axial and radial displacement rate behaviors at the outer surface.
- These linear behaviors may be due to the nature of the tensile second stage creep and rate and time dependent small deformations.
- So, prediction of the axial and radial displacement rate behaviors at the outer surface of the short fiber composites is very significant for better designing composites in the creep of the optoelectronic/photonic composite devices with optical fiber.

References

[1] H. Fukuda, T. W. Chou, J. Compos. Mater. **1**(15), 79 (1981).
[2] D. M. McClung, J. Can Geotech, Int. J. Rock. Mech. Min. Sci. Geomech. Abstracts. **20**(5), 167 (1983).
[3] M. McLean, Compos. Sci. Technol. **23**, 37 (1985).
[4] Y. S. Lee, T. J. Batt, P. K. Liaw, Int. J. Mech. Sci. **32**(10), 801 (1990).
[5] J. Zhang, Compos. Sci. Technol. **63**(13), 1877 (2003).
[6] V. Monfared, Res. J. Appl. Sci. Eng. Technol. **4**(18), 3516 (2012).
[7] Q. Zhou, Q. Zhu, C. Wei, J. Lu, L. Moraru, A. Biswas, Optoelectron. Adv. Mater. -Rapid Comm. **8**(11-12), 995 (2014).
[8] V. Monfared, D. Fazaeli, S. Daneshmand, N. Shafaghatian, Ind. J. Sci. Technol. **7**(2), 180 (2014).
[9] A. Levy, J. M. Papazian, Acta. Metall. Mater. **39**(10), 2255 (1991).
[10] K. J. Kim, W. R. Yu, M. S. Kim, Compos. Sci. Technol. **68**(7–8), 1688 (2008).
[11] W. J. Lee, J. H. Son, I. M. Park, Y. H. Park, Comput. Mater. Sci. **48**(4), 802 (2010).
[12] T. Morimoto, T. Yamaoka, H. Lilholt, M. Taya, J. Eng. Mater. Technol. **110**, 70 (1988).
[13] D. W. Meyer, R. F. Cooper, M. E. Plesha, Acta. Metall. Mater. **41**(11), 3157 (1993).
[14] L. Miu, D. Miu, Supercond. Sci. Technol. **23**(2), 1 (2010).
[15] Z. Jianfang, Y. Xiaobin, H, Ning, Procedia Engineering, **26**, 1526 (2011).
[16] X. Yang, Y. Sun, D. Shi, J. Non-Cryst. Solids. **358**(3), 519 (2012).
[17] A. R. A. Rashid, P. S. Menon, S. Shaari, Optoelectron. Adv. Mater.-Rapid Comm. **7**(11-12), 835 (2013).
[18] V. Monfared, S. Daneshmand, Kovove. Mater. http://www.kovmat.sav.sk/abstract.php?rr=53&cc=2&ss=60, In press, 53(2), (2015).

*Corresponding author: vahid_monfared@alum.sharif.edu, vahid_monfared_57@yahoo.com,